



HAL
open science

Briquettes Production from Olive Mill Waste under Optimal Temperature and Pressure Conditions: Physico-Chemical and Mechanical Characterizations

Saaida Khlifi, Marzouk Lajili, Saoussen Belghith, Salah Mezlini, Fouzi Tabet, Mejdı Jeguirim

► **To cite this version:**

Saaida Khlifi, Marzouk Lajili, Saoussen Belghith, Salah Mezlini, Fouzi Tabet, et al.. Briquettes Production from Olive Mill Waste under Optimal Temperature and Pressure Conditions: Physico-Chemical and Mechanical Characterizations. *Energies*, 2020, 13 (5), pp.1214. 10.3390/en13051214 . hal-03533703

HAL Id: hal-03533703

<https://hal.science/hal-03533703>

Submitted on 18 Jan 2022

HAL is a multi-disciplinary open access archive for the deposit and dissemination of scientific research documents, whether they are published or not. The documents may come from teaching and research institutions in France or abroad, or from public or private research centers.

L'archive ouverte pluridisciplinaire **HAL**, est destinée au dépôt et à la diffusion de documents scientifiques de niveau recherche, publiés ou non, émanant des établissements d'enseignement et de recherche français ou étrangers, des laboratoires publics ou privés.

Article

Briquettes Production from Olive Mill Waste under Optimal Temperature and Pressure Conditions: Physico-Chemical and Mechanical Characterizations

Saaida Khlifi ¹, Marzouk Lajili ¹ , Saoussen Belghith ², Salah Mezlini ², Fouzi Tabet ³ and Mejdı Jeguirim ^{4,5,*} 

¹ Ionized and Reactive Media Studies Research Unit (EMIR), Preparatory Institute of Engineering Studies of Monastir (IPEIM), University of Monastir, Monastir 5019, Tunisia; saaida.khlifi@ipeim.rnu.tn (S.K.); marzouk.lajili@ipeim.rnu.tn (M.L.)

² Mechanical Engineering Laboratory, National Engineering School of Monastir (ENIM), University of Monastir, Monastir 5019, Tunisia; belghith.saoussen@enim.rnu.tn (S.B.); salah.mezlini@enim.rnu.tn (S.M.)

³ Institut de Combustion Aérodynamique Réactivité et Environnement, UPR3021 CNRS, Université d'Orléans, 45100 Orléans, France; Fouzi.tabet@univ-orleans.fr

⁴ Institute des Sciences de Matériaux de Mulhouse, Université de Haute Alsace, 68093 Mulhouse, France

⁵ Institut de Science des Matériaux de Mulhouse (IS2M), Université de Strasbourg, 67081 Strasbourg, France

* Correspondence: mejdi.jeguirim@uha.fr; Tel.: +33-389336729

Received: 12 February 2020; Accepted: 2 March 2020; Published: 6 March 2020



Abstract: This paper aims at investigating the production of high quality briquettes from olive mill solid waste (OMSW) mixed with corn starch as a binder for energy production. For this purpose, different mass percentages of OMSW and binder were considered; 100%-0%, 90%-10%, 85%-15%, and 70%-30%, respectively. The briquetting process of the raw mixtures was carried out based on high pressures. Physico-chemical and mechanical characterizations were performed in order to select the best conditions for the briquettes production. It was observed that during the densification process, the optimal applied pressure increases notably the unit density, the bulk density, and the compressive strength. Mechanical characterization shows that the prepared sample with 15% of corn starch shows the best mechanical properties. Moreover, the corn starch binder affects quietly the high heating value (HHV) which increases from 16.36 MJ/Kg for the 100%-0% sample to 16.92 MJ/Kg for the 85%-15% sample. In addition, the kinetic study shows that the binder agent does not affect negatively the thermal degradation of the briquettes. Finally, the briquettes characterization shows that the studied samples with particles size less than 100 μm and blended with 15% of corn starch binder are promising biofuels either for household or industrial plants use.

Keywords: olive mill solid wastes; natural binder; densification; compressive strength; Physico-chemical properties; kinetic parameters

1. Introduction

Biomass feedstocks are recognized as a green energy source since their use for biofuels production could minimize significantly the greenhouse gaseous emissions generated by fossil fuels consumption [1,2]. Indeed, different alternative solid biofuels such as pellets [3,4], briquettes, or logs [5–7] can be produced from different biomass resources. These alternative fuels could be used for various thermochemical conversion processes including pyrolysis, combustion, and gasification [7–10]. In addition, liquid alternative biofuels such as biodiesel and bioethanol can be synthesized using biochemical conversion and extraction techniques [11,12]. Hence, biomass resources coming from agricultural residues, plants, and agri-food by-products are still considered as important bioenergy

sources [13,14]. Indeed, after coal and oil the biomass occupies the third place in the energy mapping worldwide [15]. Since the olive mill solid waste (OMSW) is abundant in the Mediterranean basin, leader countries such as Spain, Italy, Greece, and Tunisia have the advantage of valorizing this lignocellulosic biomass type for the energy recovery. It is to be highlighted that the OMSW is produced in an inhomogeneous phase and composed by two or three components (pulp, pits, and olive mill wastewater) depending on a two/three-phase separation process [16,17]. Furthermore, the OMSW composition (organic and inorganic compounds) varies significantly according to the soil cultivation, the rainfall, the degree of ripening, the olive variety, the climatic conditions, the use of pesticides and fertilizers, and also to the trees aging [18,19].

In order to increase the bulk density, the densification process is highly recommended. This technique will not increase only the energy density of pellets/briquettes or logs, but also permit their easy handling, loading, transportation, and storage [20,21]. In addition, for improving the mechanical properties of these solid biofuels it is highly recommended to add carefully other materials as binders such as molasses, starch, and tars [22]. The binder agent is expected to influence certain mechanical properties such as the mechanical strength, the high or low resistance to the compressions, and the low friability index [23]. However, it is necessary to select a binder that could not affect negatively the HHV, the volatile, and the ash contents.

In the literature, few studies have examined the (OMSW) briquetting [24]. Although the availability of these studies, the difference in OMSW characteristics, encourage researchers from each country to conduct their own research in order to optimize the conversion of these wastes into biofuels. Therefore, this investigation is focused on the optimization of the OMSW based briquettes preparation when using a natural binder. The optimized production conditions are selected after the Physico-chemical and mechanical properties determination according to standard methods.

2. Materials and Methods

2.1. Materials Preparation

The OMSW was collected from the Zouila Company (Mahdia, Tunisia) specialized in the second extraction of residual oil in raw OMSW and soap manufacturing situated in the region of Mahdia (Tunisia). Initially, the (OMSW) was dried and the residual oil (3%–5%) was extracted. The raw OMSW can be separated into olive pomace (OP) and olive pits (seeds). It is worth noting that only OP was used in this present study. Before, the densification stage, the raw biomass particles was grinded and sieved into finer particles ($<100\ \mu\text{m}$) in order to ensure more homogeneity. For this purpose, a Hommer Coeffe and spice Grinder mill (Serial N^o. 011. 037. 001; ARTNO: 11. 37. 1) was used. Different machines and techniques for the compaction process can be used such as the pelletizing machines, the piston press machines, the screw press, and the roller press machines. All these technologies involve the application of attractive forces between individual particles, formation of solid bridges, capillary pressure, interfacial forces, adhesive and cohesive forces, and mechanical interlocking bonds [23]. As it was reported in the literature, the reduction of the particle sizing increases the material porosity and the number of contact points for inter-particle bonding in the compaction process [25]. Furthermore, the smaller the particle sizes of sample, the lower the relative change in the length of samples as it was mentioned [26]. Hence, the obtained powder of OP was mixed with the corn starch for different mixture compositions; 100%-0%, 90%-10%, 85%-15%, and 70%-30%, respectively. Figure 1 shows the OMSW dried, the corn starch binder and their mixture in the composition 85%-15%. It is to be highlighted that added water to the mixture (up to around 20% moisture dry basis) is preferred in order to produce cohesive forces between the particles which favorite the agglomeration.

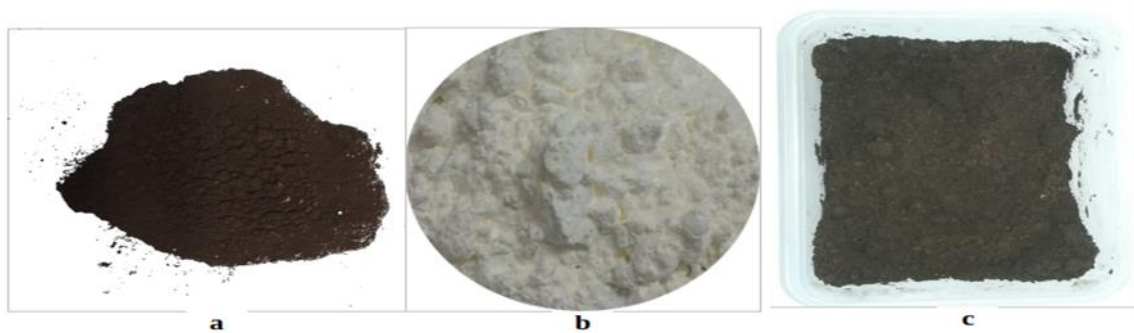


Figure 1. The used materials for the briquettes preparation: (a) Olive pomace, (b) corn starch, and (c) the mixture 85%-15%, respectively.

2.2. *Densification and Briquettes Production*

The thermal-mechanical press process is based on Gottfried Joos Maschinenfabrik GmbH & Co. machine (Stuttgart, Germany). The KG type LAP-100 with limit compression capacity of 1000 kN was chosen for briquettes production. This machine was associated to a specific mold composed of eight cylindrical imprints as it is shown (Figure 2). Every time, the cavity of the imprints should be fulfilled with the same quantities of the mixture and should be leveled off at the top to obtain a smooth surface. The moving down base of the pressing machine rises up the mold. The equipment was placed under a fixed pressure via the control valve for an optimal residence time of 15 min until obtaining the desired briquettes. The machine was wrapped with a heating element for working at a desired temperature. In this case, the samples were prepared at a low temperature of 38 °C in order to forbidden any migration of the extractives such as the residential oil or other low molecular weight molecules to the particle surface and also, to prevent the adhesion mechanisms of the Van der Waals forces causing low briquettes strengths [27]. In order to test the pressure effect on the samples, three pressures values; 100, 125, and 150 MPa were considered. The temperature was maintained at 38 °C for a residence time of 15 min according to the literature data for the commercial pelletization [28]. After the densification process, the obtained wet briquettes were extruded and dried during two weeks at the laboratory conditions (the temperature room was 28 ± 3 °C). Moreover, the densification process depends not only on the particle sizes, the fiber strength of the material, the abrasive components, but also on whether we use or not an additive binder. That is why different briquettes composed of different blends of OP and corn starch were produced. It is to be highlighted that the briquetting process uses different apparatus by comparison to the pelletizing process. Indeed, with briquettes we can go more with the pressure under which samples were prepared. However later, during the energy conversion, pellets give us more freedom for using combustion chambers with different geometries and different feeding systems than briquettes which are more suitable for fixed bed chambers.



Figure 2. The used mould die for the briquetting process.

2.3. Proximate Analysis

The proximate analysis of the prepared samples was conducted following the thermogravimetric analysis (TG) technique by using the thermal analyzer NETZSCH, model STA 449 F3, Jupiter (STA 449 F3, NETZSCH-Gerätebau GmbH, Selb, Germany) Hence, about 50 mg of each sample should be placed in a platinum. First, the initial temperature of 29 °C was maintained for 10 min, and then the samples were heated up to 950 °C at a constant heat rate of 10 °C·min⁻¹ under an inert atmosphere of nitrogen with a flow rate of 79 mL/min after reaching the maximum temperature. After that, the temperature should be decreased to 550 °C with a heating rate of 40 °C·min⁻¹. Thereafter, an oxidative atmosphere by supplying 21% oxygen flow rate was supplied. This protocol, allows extracting from the TG curve, moisture, volatiles matters (VM), fixed carbon (FC), and ash contents.

The high heating value (HHV) is the amount of heat released when the sample fuel is completely burnt with oxygen in a calorimeter bomb. For this goal, the HHV was determined based on the ASTM D5865 standards. The parr 1341 oxygen bomb calorimeter was first calibrated using a standard sample of benzoic acid whose known calorific value is 26.4 kJ/kg. A mass of about 1g of the different samples should be used. The bomb should be fulfilled of oxygen under 30 bars. By measuring the variation of temperature, the HHV can be calculated using the following expression:

$$\text{HHV} = \frac{W\Delta T - e_1 - e_2 - e_3}{m} \quad (1)$$

where ΔT is the net temperature rise, W is the equivalent energy of the calorimeter determined under standardization, e_1 represents the correction (in calories) for the heat of formation of nitric acid (HNO_3), e_2 represents the correction (in calories) for heat of formation of sulfuric acid (H_2SO_4), e_3 corresponds to the correction (in calories) for the heat of combustion of the fuse wire, and m is the weight of the tested sample.

2.4. Measurement of the Compressive Strength

The compressive strength is a significant parameter in the evaluation of the solid biofuels. This parameter is in relation with the rigidity and durability which make the biofuels storage easier [29]. In order to evaluate the compression resistance as a function of the applied pressure on prepared samples using the Lloyd Instruments (EZ20, AMETEK Company, Berwyn, UK), tests were conducted with the load speed of 1 mm/min [30]. The flat surface of the briquette sample should be placed on the horizontal metal plate of the machine. Then, an increased load is applied at a constant rate until reaching the sample's break. The maximum crushing load force that a briquette can withstand before cracking or breaking corresponds to the so-called compressive strength [27,31].

3. Results and Discussions

3.1. Compressive Strength Measurement

Figure 3 shows that the load required to the briquettes rupture for different binder ratios is significantly different. Table 1 exhibits the compressive strength of biomass briquettes produced at different pressure levels and different binder contents. Indeed, the compressive strength exhibits maximum of 4015 and 4581 kN in the case of the 85%-15% sample when imposing 125 and 150 MPa, respectively. Moreover, it is very remarkable that the compressive strength falls significantly when increasing the binder content (30%) in the samples. This result proves that the starch corn gets its maximum efficiency at 15%. Moreover, for the 100 MPa imposed pressure, the 100%-0% sample shows the highest compression strength (1581 kN) and on the contrary the compressive strength decreases significantly when increasing the binder percentage.

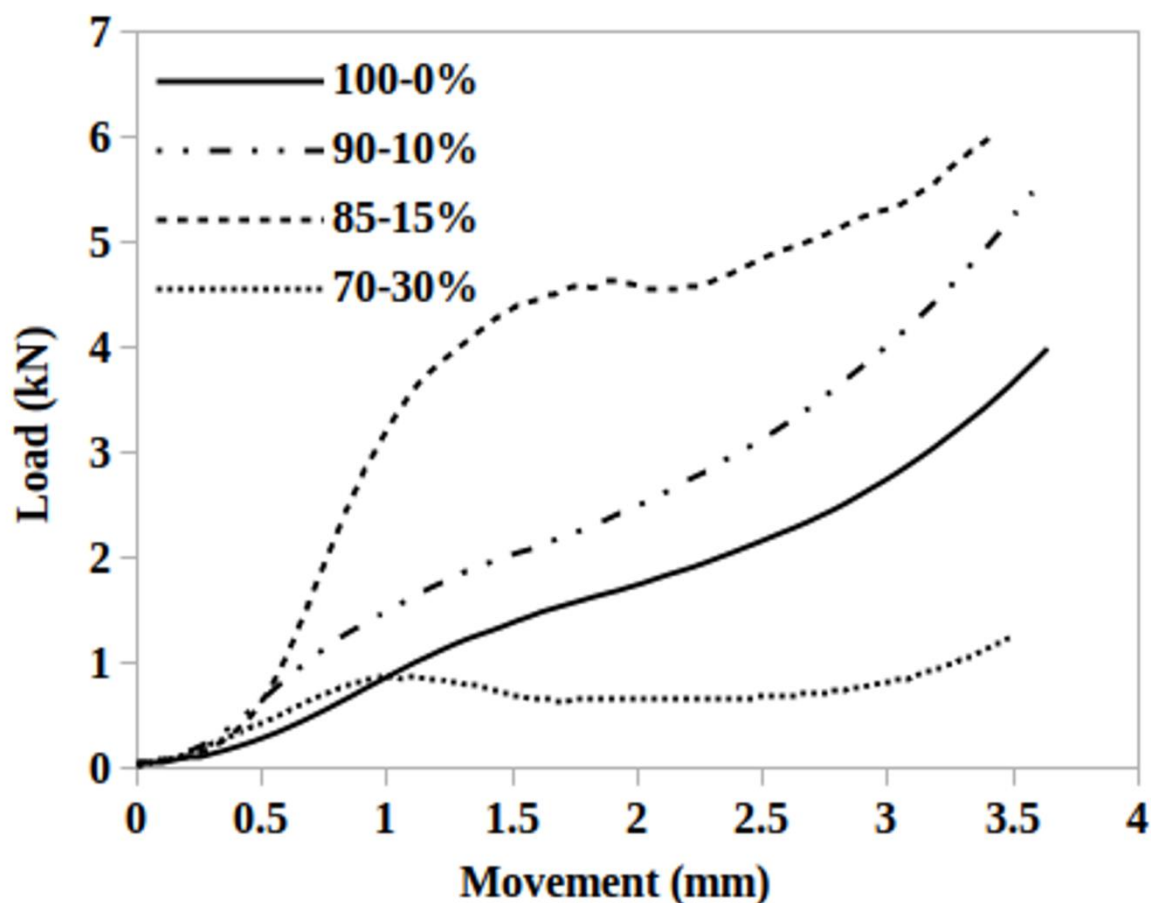


Figure 3. Variation of the load as a function of the displacement.

Table 1. Compressive strength of biomass briquettes produced at different pressure levels and different binder contents.

Pressure (MPa)	100				125				150			
Binder (%)	0	10	15	30	0	10	15	30	0	10	15	30
Compressive Strength (kN)	1581	1039	775	626	1506	1770	4015	130	1557	2090	4581	863

3.2. The Unit Density and the Bulk Density Measurements

Table 2 presents the unit density and the bulk density values of the different briquettes types when prepared at different binder percentages and at different pressure values. The unit density is the averaged ratio of the mass by the volume of each sample. Given that the briquettes are cylindrical, we should determine the mass, the radius, and the height of each sample then, by simple calculation the unit density is calculated as:

$$\rho_u = \frac{m}{V} \quad (2)$$

Table 2. Unit and bulk density of biomass briquettes produced at different pressure and different binder contents.

Pressure (MPa)	100				125				150			
Binder (%)	0	10	15	30	0	10	15	30	0	10	15	30
Unit Density (kg/dm ³)	2.04	2.83	2.81	2.31	2.41	2.40	2.47	*	2.77	2.84	2.95	3.03
Bulk Density (kg/dm ³)	0.84	0.86	0.88	0.84	0.92	0.93	0.95	*	0.95	0.98	1.20	1.10

However, the bulk density is calculated as the ratio of the briquettes mass when fulfilling a container whose volume is known and proceeding conformingly to the CEN TS15103 standard method [32]. Results indicate that the unit density values of our samples are ranging between 2.04 and 3.7 kg/dm³. These values seem to be relatively high. This can be explained by the effect of the small particle size, the low moisture content, and also by the high applied pressure [20]. Moreover, the effect of the imposed pressure on the briquettes density is foreseeable when evolving from 100 to 150 MPa. In addition, when increasing the percentage of the binder from 10% to 30% the briquettes unit density grows from 2.8 to 3.0 kg/dm³ in the case of 150 MPa imposed pressure, whereas, the briquettes bulk density exhibits a small increase from 0.95 to 1.10 kg/dm³ and 1.20 kg/dm³ as a maximum value for the 85%-15% sample. This can be explained by the fact that the corn starch particles might have played an important role in fulfilling the void between the particles which increases the inter-particle bonding. Fortunately, the unit density values of the two briquettes types are higher than the minimum value (1.12 Kg/dm³) claimed by the European standard EN14961-2 during the household use [33].

3.3. High Heating Value Measurement

Table 3 shows the proximate analyses of the prepared briquettes compared with those reported in the literature for other biomass fuels. It can be noticed that the ash content decreases due to the blending operation from 9.49% to 6.72%, but remains relatively higher than the acceptable limit (5%) of European standards. However, the produced ash by combustion for example can be reused for the brick manufacturing. Indeed, the addition of this ash type to bricks preparation helps in terms of reducing thermal conductivity, as it was stated by Eliche-Quesada and Leite-Costa [34]. Moreover, the 85%-15% sample exhibits quite an increase for the HHV which remains within the range of European norms

(>16.5 MJ.kg⁻¹) [35]. This can be justified by the quite increase of the VM content during the binder addition [36].

Table 3 also reported the proximate analysis of different biomass from the literature. We remark that the HHV of our prepared samples are lower than the HHV of the pulp (dry basis) or the pomace (except the very wet pomace with 49% moisture content). This may be due to a higher proportion of oxygen and hydrogen, and less carbon. Indeed, Munir et al. [37] found that the amount of energy contained in carbon–oxygen and carbon–hydrogen bonds is lower than in carbon–carbon bonds. The higher oxygen content in the biomass indicates that it will have a higher thermal reactivity than the other biomass [38]. Moreover, Chouchene et al. [39] tested the influence of particle size on combustion properties. They concluded that the more the particles were small, the more they were reactive. In addition, samples having less than 0.5 mm size released a high quantity of volatile matters which is in accordance with the low quantity of produced char. However, the residual ash amounts left during the oxidative pyrolysis of the olive solid wastes increase when decreasing the particle size [40]. Furthermore, using small particle sizing induces no temperature gradient leading to heat transfer limitations [40].

Table 3. Proximate analysis of prepared samples and others from literature.

Biofuels	VM (%wt)	FC (%wt)	Moisture (%wt)	Ash (%wt)	HHV (MJ/kg)
100%-0% (w.b.)	61.86	18.75	9.88	9.49	16.36
85%-15% (w.b.)	64.65	18.39	10.44	6.72	16.92
Pulp [41] (d.b.)	79.10	15.30	6.5	5.60	23.39
OP [42] (d.b.)	65	29.6	10	5.4	*
Dry OP [43] (d.b.)	86.71	7.48	4.52	5.81	19.88
Wet OP [44] (d.b.)	42.35	7.79	49.02	0.84	5.70

w.b.: wet basis; d.b.: dry basis.

3.4. Thermogravimetry Analysis

Figure 4a shows the TG curve as a function of time obtained during slow pyrolysis and followed by the char oxidation for both samples 0%-100% and 85%-15% prepared at 150 MPa, respectively. Figure 4b corresponds to the TG curve as a function of temperature during only the pyrolysis process. Figure 4a can be divided into three steps: The first step corresponds to a mass loss representing mainly the moisture evaporation up to 120 °C. The second step characterizes the devolatilization zone in which the volatiles organic compounds (VOC) are released from the hemicelluloses and a part of the lignin thermal degradation followed by the cellulose degradation. The VOC gas mixture is mainly composed by CH₄, CO₂, CO, H₂ and some traces of other C_nH_m. The second step ended by the rest of lignin degradation yielding to the char formation which is a mixture of fixed carbon and ash. The final step (Step 3 on Figure 4a) corresponds to the char oxidation when injecting oxygen and the temperature is fixed equal to 550 °C. This step ends when obtaining only ash. The obtained curve presents the same behavior as similar works reported in the literature [17,45,46].

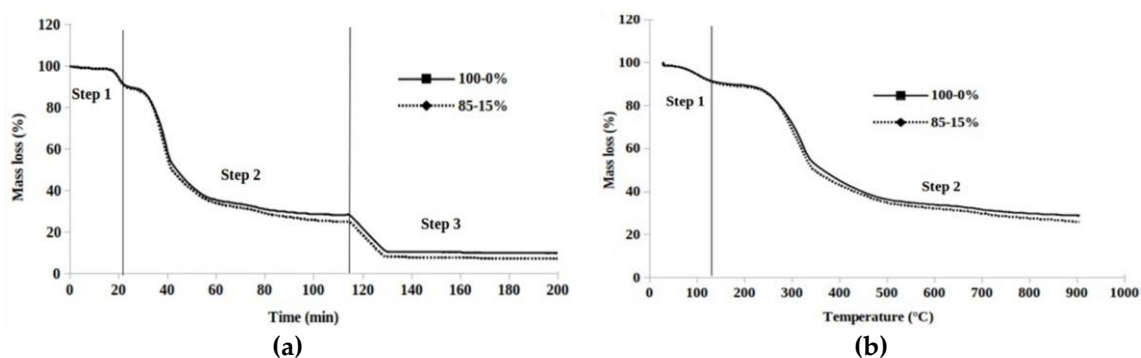


Figure 4. (a) TG curve of the 85%-15% and 100%-0% briquettes as a function of the time during pyrolysis step followed by the char oxidation (Step 3); (b) TG curve of the 85%-15% and 100%-0% briquettes as a function of the temperature during only pyrolysis step.

Figure 5 exhibits the derivative versus time of TG curves called (DTG) curves. These curves correspond to the thermal degradation under inert atmosphere of the 100%-0% and the 85%-15% samples respectively. Each one of the superposed curves shows fourth peaks with a different maximum rate of mass loss. The first peak corresponds mainly to the moisture release. Moreover, it can refer to an early stage of residual oil evaporation and light VOC degradation (below 200 °C) [47]. The second one, which is more intense occurring between 200 and 350 °C, is attributed to the hemicelluloses and cellulose degradation. In the present case, the thermal degradation of cellulose dominates the chemistry of pyrolysis (the cellulose content can be three times that of hemicelluloses; 42% and 14%, for example) [48,49]. This causes the replacement of the peak corresponding to the hemicelluloses by a shoulder (observed at the vicinity of 270 °C in our case).

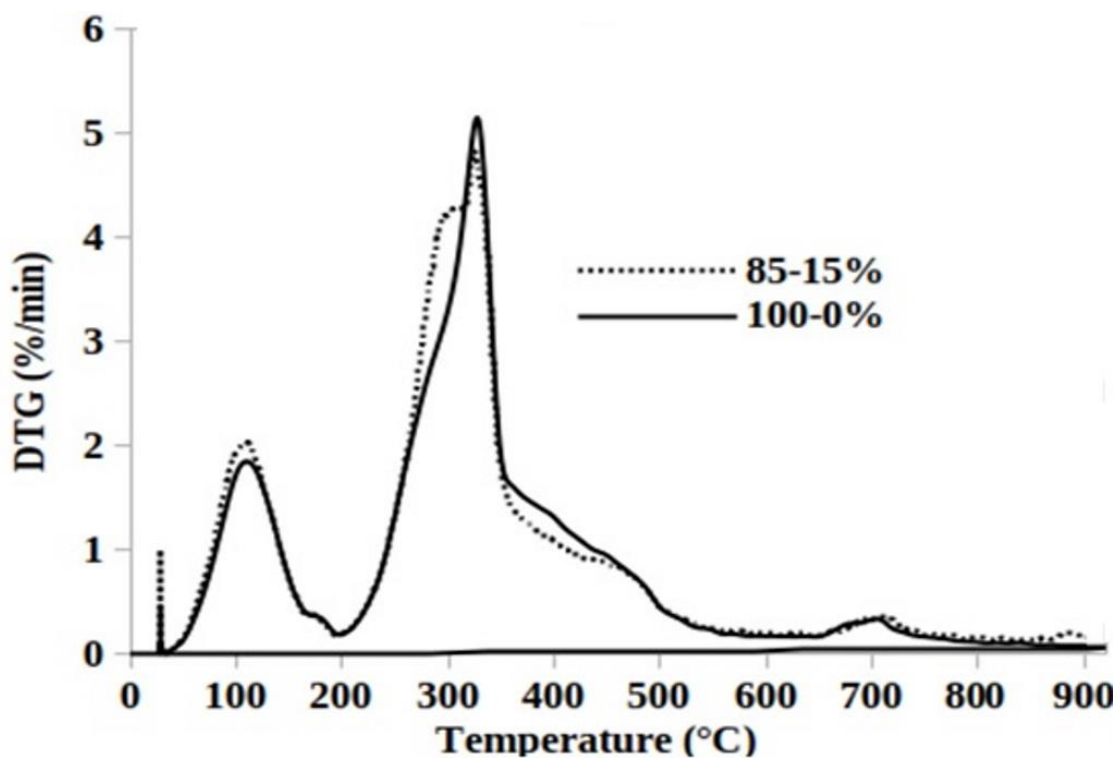


Figure 5. DTG evolution as a function of the temperature.

A similar result was reported by Ghouma et al. [46]. They observed two peaks occurring at 267 and 337 °C corresponding to the thermal decomposition of the hemicelluloses and the cellulose. The third

peak appearing at about 425 °C corresponds to the lignin and cellulose thermal degradation [50]. The final peak, occurring at the vicinity of 708 °C, is attributed to the rest of the lignin thermal degradation. Indeed, the lignin thermal degradation is in reality widely spread between 433 and 900 °C [51]. More precisely, serial shoulders have been seen for the Xylan pyrolysis in the range of 350 and 550 °C, and can be attributed to the remaining lignin [52]. It is to be highlighted that the second peak observed for the 85%-15% sample near 295 °C corresponds to the corn starch material. The Pyrolysis process corresponding to the decomposition of the hemicelluloses, the cellulose, and the lignin yields to the char formation. This remaining char will be oxidized in the following step. Indeed, during the char oxidation at 550 °C, the increased porosity of the char particles permits more diffusion of the oxygen. Therefore, the readily combustible part of lignin could react with the diffusing oxygen, even though the reactivity of lignin was low [53].

3.5. Mean Reactivity during Pyrolysis and Char Oxidation

Taking into consideration the fact that the peak intensity is directly proportional to the reactivity R_{DTG} [54], while the corresponding temperature is inversely proportional to the reactivity T_{DTG} [55], the mean reactivity R_M of each sample can be easily calculated, when considering all peaks and shoulders appearing on the DTG curves, using the following expression:

$$R_M = 100 \frac{\sum R_{DTG}}{T_{DTG}} \quad (3)$$

As it is mentioned in Table 4, the 85%–15% sample for which the DTG curve exhibits the highest value displayed the highest reactivity. This may be due to the increase of the surface area, and therefore to a higher concentration of carbon active sites per unit weight. The effect of the heating rate was previously studied [46]. Moreover, as it was stated by Qiang et al. [56] and Tenfei et al. [57], the use of binder in pellets preparation ensures lower ignition temperature, wider temperature interval, and higher oxidation activity. More precisely, when using lignin and $\text{Ca}(\text{OH})_2$ the produced pellets show lower compression energy consumption, moisture uptake, enhanced mechanical strength, and promoted combustion performance. It was found that a high heat flux in a high heating regime intensified the Boudouard reaction, while delayed the thermal decomposition of the studied biomass. This is may be due to the combined effects of the heat transfer at the different heating rates and also to the kinetics of gasification. In fact, with the low heating rate ($10 \text{ }^\circ\text{C}\cdot\text{min}^{-1}$) in this study, the initial reaction temperature and the maximum gasification rate were decreased compared to other reported studies [55]. It is necessary to point out that the yield of carbon monoxide produced did not change significantly [55].

Table 4. Determination of the mean reactivity of the biofuels during the pyrolysis and the char combustion.

Samples	Thermal Degradation	Peaks of Temperature (°C)	R_{DTG} ($\text{mg}\cdot\text{min}^{-1}$)	R_M ($\% \cdot \text{min}^{-1} \cdot ^\circ\text{C}^{-1}$)
100%-0%	Pyrolysis	118-180-329-398-448-	0.896-0.176-2.582-0.672	0.897
	Char Combustion	537-544-548	0.636-0.635-0.590	0.228
85%-15%	Pyrolysis	102-180-295-319-458-707-882-904-902	1.039-0.167-2.149-2.460-0.424-0.182-0.108-0.043-0.028	1.199
	Char Combustion	593-568-552	0.660-0.661-0.598	0.227

3.6. Kinetic Study and Pyrolysis Parameters Determination

The kinetic study of the pyrolysis process for both studied samples (100%-0% and 85%-15%) was carried out on the hypothesis where the solid-state material was heated at a constant heating rate;

$\beta = \frac{dT}{dt}$ equal to 10 K min^{-1} . This condition was widely considered in the literature [4,32,46,58,59]. This technique uses the combined kinetics three-parallel-reaction (CK-TPR) model. In the present study, a single step reaction mechanism (Equation (4)) was assumed to describe the pyrolysis kinetics of the lignocellulosic biomass. Isoconversional methods are believed to estimate the apparent activation energy (E) and the pre-exponential factor (A), when the rate of the mass loss is related to the mass and to the temperature according to Equation (5).



$$d\alpha/dT = K(T) \cdot f(\alpha) = \frac{A}{\beta} \cdot \exp\left(\frac{-E_a}{RT}\right)(1-\alpha)^n \quad (5)$$

where A denotes the pre-exponential factor (s^{-1}), E_a is the activation energy (kJ/mol), R is the ideal gas constant ($R = 8.31 \text{ J}\cdot\text{mol}^{-1}\cdot\text{K}^{-1}$), T is the temperature (K), t is time (s), α is the conversion rate varying between 1 and 0, and n is the reaction order.

The distributed activation energy model (DAEM) assumes infinity irreversible first order reactions ($f(\alpha) = 1-\alpha$) happening independently during the solid-state pyrolysis [60]. Moreover, based on the Coats-Redfern method, Equation (5) could be written as the following [61]:

$$\ln\left(\frac{-\ln(1-\alpha)}{T^2}\right) = \ln\left(\frac{A R}{\beta E_a}\right) - \frac{E_a}{R T} \quad (6)$$

Figure 6 shows the variation of $Y = \ln\left(\frac{-\ln(1-\alpha)}{T^2}\right)$ versus $X = \frac{1}{T}$. It is to be noticed that an increase of temperature yields to an increase of Y . This result is may be due to the change in pyrolytic mechanisms so that different stages could be observed with the two sample types (100%-0% and 85%-15%) [58]. The apparent activation energy (E_a) and the pre-exponential factor (A) were calculated using the slopes of the linear trends of the curve and all results were consigned in Table 5.

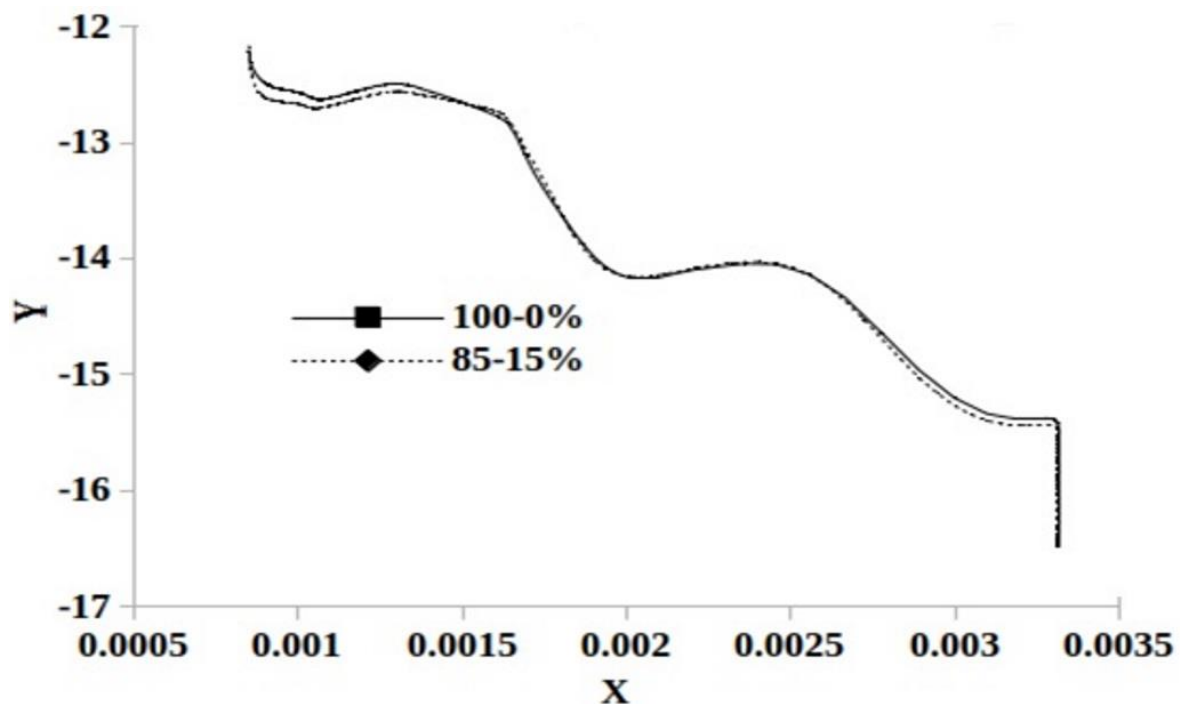


Figure 6. Kinetic analysis during the thermal decomposition of the 85%-15% and 100%-0% samples. The activation energy is calculated from the slope of linear trends.

Table 5. Kinetic parameters determination during the nonisothermal pyrolysis.

Samples	Range of Temperature (°C)	Linear Equation	Ea (kJ·mol ⁻¹)	A (min ⁻¹)
85%-15%	54–126	$f(x) = -2518.82x - 7.707$	20.94	11.32
	135–225	$f(x) = 343.72x - 14.85$	n.d.	n.d.
	230–353	$f(x) = -4201.99x - 5.98$	34.93	106.26
	360–438	$f(x) = -595.3x - 11.77$	4.94	0.05
100%-0%	60–134	$f(x) = -2232.08x - 8.47$	18.55	4.38
	151–225	$f(x) = 376.062x - 14.93$	n.d.	n.d.
	235–368	$f(x) = -3895.77x - 6.558$	32.38	55.27
	378–498	$f(x) = -898.09x - 11.3$	7.46	0.11

n.d.: not determined

Table 5 shows that the activation energy of the 85%-15% sample for different pyrolysis steps were 20.94, 34.93, and 4.94 kJ·mol⁻¹. The activation energy reaches its maximum during the hemicelluloses and cellulose decomposition. It was concluded that the activation energies present relatively low values, which could be due to the small particle, so that the pyrolysis reactions start at low temperatures. The 85%-15% sample presents a less range of temperature during the decomposition of the three main components than the 100%-0% sample, and this is the reason of the higher reactivity [62]. Moreover, we can notice that, when moving from the first to the second stage, the temperature increases and the activation energy takes a maximum value. At this stage the higher activation energy refers to the diffusing effect of volatiles and gas. Then, when moving from the second to the third stage it is notable that the activation energy decreases. This means that the chemical reaction becomes easier. Similar trends of this activation energy evolution were reported in the literature [63].

4. Conclusions

In this work, we studied the mechanical properties and the thermal-chemical properties of biofuels briquettes. Two sorts blended with a natural binder and non-blended briquettes were densified under a high pressure. The results we obtained show that the briquettes produced from olive pomace blended with corn starch as a binder can be densified into high quality briquettes showing acceptable parameters for a future thermal use. Indeed, the proximate analysis of the prepared briquettes, show less moisture contents. Moreover, the addition of corn starch as a natural binder conducts an improvement on the sample's compressive strength, as well as to a reduction of the ash content and to a quite increase of the high heating value. TG tests were carried out followed by a kinetic study for the two samples 100%-0% and 85%-15%. We concluded that the binder increases the thermal degradation of the briquettes during the nonisothermal pyrolysis, while increasing the activation energy. Next, a numerical simulation and modeling of the combustion of pyrolysis VOC in a cocurrent reactor will be conducted using the OpenFOAM software (18.12+, OpenCFD Limited, Bracknell, UK).

Author Contributions: Conceptualization, M.L. and S.M.; Methodology, M.L. and M.J.; Formal Analysis, M.L. and S.B.; Investigation, M.L., F.T. and M.J.; Resources, M.L. and S.M.; Data Curation, S.K., M.L. and S.M.;

Writing-Original Draft Preparation, S.K., S.B. and M.L.; Writing-Review & Editing, M.L. and M.J.; Supervision, M.L.; Project Administration, M.L. All authors have read and agreed to the published version of the manuscript.

Funding: This research received no external funding.

Acknowledgments: Saaida Khelifi and Marzouk Lajili would like to express their thanks to Brahim Sarh and Toufik Boushaki, as well as the technical team of ICARE Laboratory of Orleans University (France) for the good technical assistance during the experimental tests realization.

Conflicts of Interest: The authors declare no conflict of interest.

References

1. Popp, J.; Lakner, Z.; Harangi-Rákos, M.; Fári, M. The effect of bioenergy expansion: Food, energy, and environment. *Renew. Sust. Energy Rev.* **2014**, *32*, 559–578. [[CrossRef](#)]
2. Demirbaş, A. Biomass resource facilities and biomass conversion processing for fuels and chemicals. *Energy Convers. Manag.* **2001**, *42*, 357–1378. [[CrossRef](#)]
3. McKendry, P. Energy production from biomass (Part 1): Overview of biomass. *Bioresour. Technol.* **2002**, *83*, 37–46. [[CrossRef](#)]
4. Limousy, L.; Jeguirim, M.; Dutournié, P.; Kraeim, N.; Lajili, M.; Said, R. Gaseous products and particulate matter emissions of biomass residential boiler fired with spent coffee ground pellets. *Fuel* **2013**, *107*, 323–329. [[CrossRef](#)]
5. Merpati Mitan, N.M.; Azmi, A.H.; Nur Fathiah, M.N.; Se, S.M. Binder application in durian peels briquette as a solid biofuel. *Appl. Mech. Mater.* **2015**, *761*, 494–498. [[CrossRef](#)]
6. Limousy, L.; Jeguirim, M.; Labbe, S.; Balay, F.; Fossard, E. Performance and emissions characteristics of compressed spent coffee ground/wood chip logs in a residential stove. *Energy Sustain. Dev.* **2015**, *28*, 52–59. [[CrossRef](#)]
7. Khelifi, S.; Lajili, M.; Tabet, F.; Boushaki, T.; Sarh, B. Investigation of the combustion characteristics of briquettes prepared from olive mill solid waste blended with and without a natural binder in a fixed bed reactor. *Biomass Convers. Bior.* **2019**. [[CrossRef](#)]
8. Fachinger, F.; Drewnick, F.; Gieré, R.; Borrmann, S. How the user can influence particulate emissions from residential wood and pellet stoves: Emission factors for different fuels and burning conditions. *Atmos. Environ.* **2017**, *158*, 216–226. [[CrossRef](#)]
9. Ferreira, S.; Monteiro, E.; Brito, P.; Vilarinho, C. A Holistic Review on Biomass Gasification Modified Equilibrium Models. *Energies* **2019**, *12*, 160. [[CrossRef](#)]
10. Zribi, M.; Lajili, M.; Escudero Sanz, R.F. Hydrogen enriched syngas production via gasification of biofuels pellets/powders blended from olive mill solid wastes and pine sawdust under different water steam/nitrogen atmospheres. *Int. J. Hyd. Energy* **2019**, *44*, 11280–11288. [[CrossRef](#)]
11. Zhang, F.; Fang, Z.; Wang, Y.T. Biodiesel production directly from oils with high acid value by magnetic $\text{Na}_2\text{SiO}_3@Fe_3O_4/C$ catalyst and ultrasound. *Fuel* **2015**, *150*, 370–377. [[CrossRef](#)]
12. Hahn-Hägerdal, B.; Galbe, M.; Gorwa-Grauslund, M.F.; Lidén, G.; Zacchi, G. Bio-ethanol—The fuel of tomorrow from the residues of today. *Trends Biotechnol.* **2006**, *24*, 12. [[CrossRef](#)] [[PubMed](#)]
13. Hamelinck, C.N.; Faaij, A.P.C. Outlook for advanced biofuels. *Energy Policy* **2006**, *34*, 3268–3283. [[CrossRef](#)]
14. Scarlat, N.; Dallemand, J.F.; Monforti-Ferrario, F.; Nita, V. The role of biomass and bioenergy in a future bioeconomy: Policies and facts. *Environ. Dev.* **2015**, *15*, 3–34. [[CrossRef](#)]
15. Sahu, S.G.; Sarkar, P.; Mukherjee, A.; Adak, A.K.; Chakraborty, N. Studies on the co-combustion behavior of coal/biomass blends using thermogravimetric analysis. *IJETAE* **2013**, *3*, 131–138.
16. Azbar, N.; Bayram, A.; Filibeli, A.; Muezzinoglu, A.; Sengul, F.; Ozer, A. A review of waste management options in olive oil production. *Crit. Rev. Env. Sci. Technol.* **2004**, *34*, 209–247. [[CrossRef](#)]
17. Ouazzane, H.; Laajine, F.; ElYamani, M.; el Hilaly, J.; Rharrabti, Y.; Amarouch, M.Y.; Mazouzi, D. Olive Mill Solid Waste Characterization and Recycling opportunities: A review. *J. Mater. Environ. Sci.* **2017**, *8*, 2632–2650.
18. Niaounakis, M.; Halvadakis, C.P. *Olive Processing Waste Management; Literature Review and Patent Survey*: London, UK, 1 February 2006.
19. Dermeche, S.; Nadour, M.; Larroche, C.; Moulti-Mati, F.; Michaud, P. Olive mill wastes: Biochemical characterizations and valorization strategies. *Process Biochem.* **2013**, *48*, 1532–1552. [[CrossRef](#)]

20. Tumuluru, J.S. Effect of process variables on the density and durability of the pellets made from high moisture corn stover. *Biosyst. Eng.* **2014**, *119*, 44–57. [[CrossRef](#)]
21. Tumuluru, J.S. Specific energy consumption and quality of wood pellets made from high moisture lodgepole pine biomass. *Chem. Eng. Res. Des.* **2016**, *110*, 82–97. [[CrossRef](#)]
22. Kaliyan, N.; Morey, R.V. Natural binders and solid bridge type binding mechanisms in briquettes and pellets made from corn Stover and switch grass. *Bioresour. Technol.* **2010**, *101*, 1082–1090. [[CrossRef](#)] [[PubMed](#)]
23. Zanella, K.; Concentino, V.O.; Taranto, O.P. Influence of the type of Mixture and Concentration of Different Binders on the Mechanical Properties of “Green” Charcoal Briquettes. *Chem. Eng. Trans.* **2017**, *57*, 199–204.
24. Christoforou, E.; Fokaides, P. A review of olive mill solid wastes to energy utilization techniques. *Waste Manag.* **2016**, *49*, 346–363. [[CrossRef](#)] [[PubMed](#)]
25. Ganvir, K.D.; Tulankar, P.G.; Bawankar, P.P.; Rahimkar, K.T.; Singh, S.L. Analysis and Comparison of Biomass Pellets with Various Fuels. *IJSRD* **2017**, *5*, 1272–1274.
26. Davies, R.M.; Davies, O.A. Effect of Briquetting Process Variables on Hygroscopic Property of Water Hyacinth Briquettes. *Hindawi Publ. Corp. J. Renew. Energy* **2013**, 1–5. [[CrossRef](#)]
27. Stelte, W.; Holm, J.K.; Sanadi, A.R.; Barsberg, S.; Ahrenfeldt, J.; Henriksen, U.B. A study of bonding and failure mechanisms in fuel pellets from different biomass resources. *Biomass Bioenergy* **2011**, *35*, 910–918. [[CrossRef](#)]
28. Adapa, P.K.; Tabil, L.G.; Schoenau, G.J.; Sokhansanj, S. Pelletizing Characteristics of Fractionated and Sun-Cured Dehydrate Alfalfa Grinds. *Appl. Eng. Agric.* **2004**, *20*, 813–820. [[CrossRef](#)]
29. Swietochowski, A.; Lisowski, A.; Dabrowska-Salwin, M. Strength of briquettes and pellets from energy crops. *Eng. Rural Dev.* **2016**, *5*, 25–27.
30. Sprenger, C.J.; Tabil, L.G.; Soleimani, M.; Agnew, J.; Harrison, A. Pelletization of Refuse-Derived Fuel Fluff to Produce High Quality Feedstock. *J. Energy Resour. Technol.* **2018**, *140*. [[CrossRef](#)]
31. Richards, S.R. Physical testing of fuel briquettes. *Fuel Process. Technol.* **1990**, *25*, 89–100. [[CrossRef](#)]
32. Lajili, M.; Limousy, L.; Jeguirim, M. Physico-chemical properties and thermal degradation characteristics of agropellets from olive mill by-products/sawdust blends. *Fuel Process. Technol.* **2014**, *126*, 215–221. [[CrossRef](#)]
33. Mehdipour, I.; Khayat, K.H. Effect of supplementary Cementitious Material Content and Binder Dispersion on Packing Density and Compressive Strength of Sustainable Cement Paste. *ACI Mater. J.* **2016**, *113*, 361–372.
34. Eliche-Quesada, D.; Leite-Costa, J. Use of bottom ash from olive pomace combustion in the production of eco-friendly fired clay bricks. *Waste Manag.* **2016**, *48*, 323–333. [[CrossRef](#)] [[PubMed](#)]
35. Eija Alakangas, V.T.T. *New European Pellets Standards*; EUBIONET 3: Swedish, Finland, March 2011.
36. Long, Y.; Meng, A.; Chen, S.; Zhou, H.; Zhang, Y.; Li, Q. Pyrolysis and Combustion of Typical Wastes in a Newly Designed Macro Thermogravimetric Analyzer: Characteristics and Simulation by Model Components. *Energy Fuels* **2017**, *31*, 7582–7590. [[CrossRef](#)]
37. Munir, S.; Daood, S.S.; Nimmo, W.; Cunliffe, A.M.; Gibbs, B.M. Thermal analysis and devolatilization kinetics of cotton stalk, sugar cane bagasse and shea meal under nitrogen and air atmospheres. *Bioresour. Technol.* **2009**, *100*, 1413–1418. [[CrossRef](#)]
38. Haykiri-Acma, H.; Yaman, S. Effect of co-combustion on the burnout of lignite/biomass blends: A Turkish case study. *Waste Manag.* **2008**, *28*, 2077–2084. [[CrossRef](#)]
39. Chouchene, A.; Jeguirim, M.; Khiari, B.; Zagrouba, F.; Trouvé, G. Thermal degradation of olive solid waste: Influence of particle size and oxygen concentration. *Resour. Conserv. Recy.* **2010**, *54*, 271–277. [[CrossRef](#)]
40. Vamvuka, D.; Kakaras, E.; Kastanaki, E.; Grammelis, P. Pyrolysis characteristics and kinetics of biomass residuals mixtures with lignite. *Fuel* **2003**, *82*, 1949–1960. [[CrossRef](#)]
41. Miranda, T.; Esteban, A.; Rojas, S.; Montero, I.; Ruiz, A. Combustion Analysis of Different Olive Residues. *Int. J. Mol. Sci.* **2008**, *9*, 512–525. [[CrossRef](#)]
42. Borello, D.; De Caprariis, B.; De Filippis, P.; Di Carlo, A.; Marchegiani, A.; Marco Pantaleo, A.; Shah, N.; Venturini, P. Thermo-Economic Assessment of a olive pomace Gasifier for Cogeneration Applications. *Energy Procedia* **2015**, *75*, 252–258. [[CrossRef](#)]
43. Alrawashdeh, K.A.b.; Slopicka, K.; Alshorman, A.A.; Bartocci, P.; Fantozzi, F. Pyrolytic Degradation of Olive Waste Residue (OWR) by TGA: Thermal Decomposition Behavior and Kinetic Study. *J. Energy Power Eng.* **2017**, *11*, 497–510.
44. Bartocci, P.; D’Amico, M.; Moriconi, N.; Bidini, G.; Fantozzi, F. Pyrolysis of olive stone for energy purposes. *Energy Procedia* **2015**, *82*, 374–380. [[CrossRef](#)]

45. Tamošiūnas, A.; Chouchène, A.; Valatkevičius, P.; Gimžauskaitė, D.; Aikas, M.; Uscila, R.; Ghorbel, M.; Jeguirim, M. The Potential of Thermal Plasma Gasification of Olive Pomace Charcoal. *Energies* **2017**, *10*, 710. [[CrossRef](#)]
46. Ghouma, I.; Jeguirim, M.; Guizani, C.; Ouederni, A.; Limousy, L. pyrolysis of Olive Pomace: Degradation kinetics. Gaseous analysis and char characterization. *Waste Biomass Valorization* **2017**, *8*, 1689–1697. [[CrossRef](#)]
47. Chiti, Y.; Salvador, S.; Commandré, J.M.; Broust, B. Thermal decomposition of bio-oil: Focus on the products yields under different pyrolysis conditions. *Fuel* **2012**, *102*, 274–281. [[CrossRef](#)]
48. Abed, I.; Paraschiv, M.; Loubar, K.; Zagrouba, F.; Tazerout, M. Thermogravimetric investigation and thermal conversion kinetics of typical North African and Middle Eastern lignocellulosic wastes. *Bioresources* **2012**, *7*, 1200–1220.
49. Shen, D.K.; Gu, S.; Bridgwater, A.V. The thermal performance of the polysaccharides extracted from hardwood: Cellulose and hemicellulose. *Carbohydr. Polym.* **2010**, *82*, 39–45. [[CrossRef](#)]
50. Varma, A.K.; Mondal, P. Physicochemical Characterization and Pyrolysis Kinetic Study of Sugarcane Bagasse Using Thermogravimetric Analysis. *J. Energy Resour. Technol.* **2016**, *138*, 11. [[CrossRef](#)]
51. Ounas, A.; Aboulkas, A.; El harfi, K.; Bacaoui, A.; Yaacoubi, A. Pyrolysis of olive residue and sugar cane bagasse: Non-isothermal thermogravimetric kinetic analysis. *Bioresour. Technol.* **2011**, *102*, 11234–11238. [[CrossRef](#)]
52. Cheng, K.; Winter, W.T.; Stipanovic, A.J. A modulated-TGA approach to the kinetics of lignocellulosic biomass pyrolysis/combustion. *Polym. Degrad. Stabil.* **2012**, *97*, 1606–1615. [[CrossRef](#)]
53. Gani, A.; Naruse, I. Effect of cellulose and lignin content on pyrolysis and combustion characteristics for several types of biomass. *Renew. Energy* **2007**, *32*, 649–661. [[CrossRef](#)]
54. Gil, M.V.; Oulego, P.; Casal, M.D.; Pevida, C.; Pis, J.J.; Rubiera, F. Mechanical durability and combustion characteristics of pellets from biomass blends. *Bioresour. Technol.* **2010**, *101*, 8859–8867. [[CrossRef](#)]
55. Vamvuka, D.; Karouki, E.; Sfakiotakis, S. Gasification of waste biomass chars by carbon dioxide via thermogravimetry. Part I: Effect of mineral matter. *Fuel* **2011**, *90*, 1120–1127. [[CrossRef](#)]
56. Hu, Q.; Shao, J.; Haiping, Y.; Yao, D.; Wang, X.; Chen, H. Effect of binders on the properties of bio-char pellets. *Appl. Energy* **2015**, *157*, 508–516. [[CrossRef](#)]
57. Wang, T.; Wang, Z.; Zhai, Y.; Li, S.; Liu, X.; Wang, B.; Li, C.; Zhu, Y. Effect of molasses binder on the pelletization of food waste hydrochar for enhanced biofuels pellets production. *Sustain. Chem. Pharm.* **2019**, *14*, 100183. [[CrossRef](#)]
58. Zribi, M.; Lajili, M. Study of the Pyrolysis of Biofuels Pellets Blended from Sawdust and Oleic by-Products: A Kinetic Study. *IJRER* **2019**, *9*, 561–571.
59. Cai, J.; Chen, Y.; Liu, R. Isothermal kinetic predictions from nonisothermal data by using the iterative linear integral isoconversional method. *J. Energy Inst.* **2014**, *87*, 183–187. [[CrossRef](#)]
60. Vyazovkin, S.; Burnham, A.K.; Criado, J.M.; Pérez-Maqueda, L.A.; Popescu, C.; Sbirrazzuoli, N. ICTAC Kinetics Committee recommendations for performing kinetic computations on thermal analysis data. *Thermochimica Acta* **2011**, *520*, 1–19. [[CrossRef](#)]
61. Wang, Y.; Sun, Y.; Wu, K. Effects of Waste Engine Oil Additive on the Pelletizing and Pyrolysis Properties of Wheat Straw. *Bioresources* **2019**, *14*, 537–553.
62. Guo, J.; Lua, A.C. Kinetic study on pyrolytic process of oil-palm solid waste using two-step consecutive reaction model. *Biomass Bioenergy* **2001**, *20*, 223–233. [[CrossRef](#)]
63. Wang, X.; Hu, M.; Hu, W.; Chen, Z.; Liu, S.; Hu, Z.; Xiao, B. Thermogravimetric kinetic study of agricultural residue biomass pyrolysis based on combined kinetics. *Bioresour. Technol.* **2016**, *219*, 510–520. [[CrossRef](#)] [[PubMed](#)]

